Localization of Piecewise Curvilinearly Moving Targets Using Azimuth and Azimuth Rates

Julian Hörst and Marc Oispuu
Fraunhofer FKIE, Dept. Sensor Data and Information Fusion
Neuenahrer Str. 20, 53343 Wachtberg, Germany
{julian.hoerst, marc.oispuu}@fkie.fraunhofer.de

Abstract: Detailed knowledge of the estimation performance for passive tracking of maneuvering targets is of fundamental interest. Therefore, the maximum achievable localization accuracy for maneuvering targets from azimuth measurements as well as from combined azimuth and azimuth rate measurements are calculated in this paper. These targets perform a piecewise curvilinear motion with an unknown number of maneuvers at unknown times. It is proven that in addition to the azimuth angles also azimuth rates contain valuable information about the kinematics of maneuvering targets that can be exploited with advantage for state estimation.

1 Introduction

State estimation of an emitting source from passive bearing measurements collected by a single moving observer is a widely investigated problem. This problem is commonly referred to as Target Motion Analysis (TMA) [Bec01] and is encountered in various fields like wireless communications, as well as airborne radar and underwater sonar applications. Aspects of the TMA problem examined in the literature include bearings-only estimation algorithms, estimation accuracy, and target observability [Bec01, Bec96].

In many cases, the targets are not moving inertially (i.e. non-accelerated), but are partly strongly maneuvering. Commonly maneuvering targets can be characterized by the so-called *curvilinear motion* model described in [BN97]. This model assumes constant and simultaneously active tangential (i.e. along-track) and normal (i.e. cross-track) accelerations a_{t} and a_{n}. An approximate solution of the curvilinear motion equation has also been presented in [BN97] for the case that the relative change of velocity is much lower than 1. The evaluation of the Cramér-Rao bound (CRB) has been realized in [RA03, RAG04] with the limiting condition that the maneuver change-over times and the maneuvers are exactly known.

In [OH10], we considered maneuvering targets performing a curvilinear motion in each maneuver segment (see Fig. 1) known as the *piecewise curvilinear motion* model established by Becker [Bec05]. It is important to emphasize that the maneuver change-over times are unknown, i.e. these parameters have to be estimated.

In contrast to [OH10], where we only investigated azimuth measurements, we consider additional azimuth rate measurements in this work. The azimuth rate can be obtained,

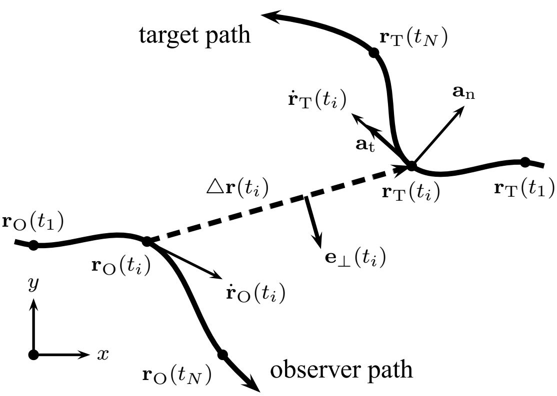

Figure 1: Scenario with an arbitrary moving sensor and a piecewise curvilinearly moving target.

e.g., by joint processing of sensor array signals. Since acquiring these quantities from raw signals is an estimation problem, the CRB of the azimuth angles and azimuth rates can be derived [WE95]. Recently, several estimation approaches have been proposed, e.g., in [MBS05] for a planar array to obtain azimuth angles, elevation angles and the corresponding rates.

2 Estimation problem

We consider the scenario depicted in Fig. 1. A maneuvering target moves along a trajectory $\mathbf{r}_\mathrm{T}(t) = (x(t), y(t))^T$ with velocity $\dot{\mathbf{r}}_\mathrm{T}(t) \in \mathbb{R}^{2\times 1}$ and constant tangential acceleration $a_\mathrm{t} = |\mathbf{a}_\mathrm{t}|$ and normal acceleration $a_\mathrm{n} = |\mathbf{a}_\mathrm{n}|$. Furthermore, a single observer moves along an arbitrary trajectory $\mathbf{r}_\mathrm{O}(t) \in \mathbb{R}^{2\times 1}$. The target observer geometry is given by the relative vector $\triangle\mathbf{r}(t) = \mathbf{r}_\mathrm{T}(t) - \mathbf{r}_\mathrm{O}(t)$ and its velocity $\triangle\dot{\mathbf{r}}(t) = \dot{\mathbf{r}}_\mathrm{T}(t) - \dot{\mathbf{r}}_\mathrm{O}(t)$. The observer's objective is to estimate the target state from passively measured line-of-sight azimuth angles α and azimuth rates $\dot{\alpha}$.

2.1 Motion model

The state of a target moving on a plane with constant tangential and normal acceleration can be completely described by the position components of $\mathbf{r}_\mathrm{T}(t)$, two velocity components of $\dot{\mathbf{r}}_\mathrm{T}(t)$ given by the velocity $v(t)$ and the course $\varphi(t)$, and the acceleration components a_t and a_n. The special cases of inertial motion ($a_\mathrm{t} = a_\mathrm{n} = 0$), straight-line acceleration ($a_\mathrm{t} \neq 0$, $a_\mathrm{n} = 0$), and circular motion ($a_\mathrm{t} = 0$, $a_\mathrm{n} \neq 0$) are included in this model. All target parameters are comprised in the parameter vector $\mathbf{x}(t) = (x(t), y(t), v(t), \varphi(t), a_\mathrm{t}, a_\mathrm{n})^T \in \mathbb{R}^{6\times 1}$. From the results of our previous work, we know that the exact solution of the motion equation has the form

$$\mathbf{x}(t) = \mathbf{f}[\mathbf{x}(t_0); t, t_0], \tag{1}$$

where (1) describes the temporally evolution of the target state from t_0 to t. The derivation of the components in (1) can be found in [OH10]. Mentionable, the initial time t_0 can be replaced by any reference time $t_\mathrm{r} > t_0$. The state at t_r can be written shortly as $\mathbf{x}_\mathrm{r} = \mathbf{x}(t_\mathrm{r})$.

In the case of piecewise curvilinear motion, the dimension of the target state $\mathbf{x}(t)$ increases by three components with each maneuver change-over. That means, two acceleration components and the maneuver change-over time are added to the target state. With M maneuvers, the augmented target state is specified by

$$\mathbf{x}(t) = \left(x(t), y(t), v(t), \varphi(t), \mathbf{a}^T, \tilde{\mathbf{t}}^T\right)^T \tag{2}$$

with $\mathbf{a} = (a_{\mathrm{t},0}, a_{\mathrm{n},0}, ..., a_{\mathrm{t},M}, a_{\mathrm{n},M})^T \in \mathbb{R}^{2+2M\times 1}$ and $\tilde{\mathbf{t}} = (\tilde{t}_1, ..., \tilde{t}_M)^T \in \mathbb{R}^{M\times 1}$. Here, $\tilde{t}_m$ is the change-over time of the m-th maneuver and $a_{\mathrm{t},m}$ and $a_{\mathrm{n},m}$ denote the tangential and normal acceleration in the time interval $[\tilde{t}_{m-1}, \tilde{t}_m]$, $m = 1, ..., M$.

Similar to (1), the target state can be parameterized by the state at another time, e.g. by $\mathbf{x}_m = \mathbf{x}(\tilde{t}_m)$. Since the reference state is commonly the current state, the state for M maneuvers in the time interval $[t_0, t_\mathrm{r}]$ is given by

$$\mathbf{x}(t) = \begin{cases} \mathbf{f}[\mathbf{x}_1; t, \tilde{t}_1] & \text{for } t_0 \le t \le \tilde{t}_1 \\ \quad\vdots & \quad\vdots \\ \mathbf{f}[\mathbf{x}_m; t, \tilde{t}_m] & \text{for } \tilde{t}_{m-1} < t \le \tilde{t}_m \\ \quad\vdots & \quad\vdots \\ \mathbf{f}[\mathbf{x}_M; t, \tilde{t}_M] & \text{for } \tilde{t}_{M-1} < t \le \tilde{t}_M \\ \mathbf{f}[\mathbf{x}_\mathrm{r}; t, t_\mathrm{r}] & \text{for } \tilde{t}_M < t \le t_\mathrm{r} \end{cases}, \tag{3}$$

where the state at some arbitrary time t is related to the reference state by

$$\mathbf{f}[\mathbf{x}_m; t, \tilde{t}_m] = \mathbf{f}[\mathbf{f}[\cdots \mathbf{f}[\mathbf{x}_\mathrm{r}; t, t_\mathrm{r}]; \cdots]; t, \tilde{t}_m]\,. \tag{4}$$

2.2 Measurement model

For the sake of simplicity, we assume that the detection probability is equal to 1 and the false alarm rate is equal to 0. The measured azimuth α_m and azimuth rate $\dot{\alpha}_\mathrm{m}$ at time t_i, $i = 1, ..., N$, are given by

$$\begin{aligned} \alpha_\mathrm{m}(t_i) &= \alpha(t_i) + w_\alpha(t_i)\,, \\ \dot{\alpha}_\mathrm{m}(t_i) &= \dot{\alpha}(t_i) + w_{\dot{\alpha}}(t_i)\,, \end{aligned} \tag{5}$$

where $w_\alpha(t_i)$ and $w_{\dot{\alpha}}(t_i)$ denote the measurement error, and

$$\begin{aligned} \alpha(t) &= \arctan \frac{\triangle x(t)}{\triangle y(t)}\,, \\ \dot{\alpha}(t) &= \frac{\triangle \dot{x}(t) \triangle y(t) - \triangle x(t) \triangle \dot{y}(t)}{\triangle x^2(t) + \triangle y^2(t)} = \frac{\triangle \dot{\mathbf{r}}^T(t)\, \mathbf{e}_\perp(t)}{\triangle r(t)} \end{aligned} \tag{6}$$

indicate the true azimuth angle and the true azimuth rate. In (6), $\triangle\dot{\mathbf{r}}(t) = (\triangle\dot{x}(t), \triangle\dot{y}(t))^T$, $\mathbf{e}_\perp(t)$ is a unit vector orthogonal to the relative vector $\triangle\mathbf{r}(t) = (\triangle x(t), \triangle y(t))^T$, and $\triangle r(t) = |\triangle\mathbf{r}(t)|$ denotes the distance between observer and target (Fig. 1). The observer state (position $\mathbf{r}_\mathrm{O}(t)$ and velocity $\dot{\mathbf{r}}_\mathrm{O}(t)$) is assumed to be exactly known. With this, the equations in (6) only depend on the target state.

We assume that the azimuth and azimuth rate measurements are independent of each other, that the measurement noise vectors are zero-mean Gaussian, and that the measurement covariances read $\mathbf{W}_\alpha = \sigma_\alpha^2\,\mathbf{I}_N$ and $\mathbf{W}_{\dot\alpha} = \sigma_{\dot\alpha}^2\,\mathbf{I}_N$. Here, σ_α^2 and $\sigma_{\dot\alpha}^2$ denote the constant noise variances and $\mathbf{I}_N$ denotes the $N \times N$-dimensional identity matrix. We note that in practice, the variances may change from time to time and have to be estimated.

With the previous considerations, the problem can be stated as follows: Estimate the target state $\mathbf{x}_\mathrm{r}$ at some reference time t_r from all measurements. We consider two measurement sets, only azimuth measurements and both azimuth and azimuth rate measurements.

3 Cramér-Rao bound (CRB)

The CRB provides a lower bound on the estimation accuracy of any unbiased estimator and its parameter dependencies reveal characteristic features of the estimation problem. Let $\mathbf{x}_\mathrm{r}$ denote an unknown parameter vector and let $\hat{\mathbf{x}}_\mathrm{r}(\boldsymbol{\psi}_\mathrm{m})$ be some unbiased estimate of $\mathbf{x}_\mathrm{r}$ based on the measurement set $\boldsymbol{\psi}_\mathrm{m}$. The CRB is given by the inverse Fisher Information Matrix (FIM)

$$\mathbf{J}_\psi(\mathbf{x}_\mathrm{r}) = \mathrm{E}\left\{\left(\frac{\partial\mathcal{L}(\boldsymbol{\psi}_\mathrm{m};\mathbf{x}_\mathrm{r})}{\partial\mathbf{x}_\mathrm{r}}\right)^T\left(\frac{\partial\mathcal{L}(\boldsymbol{\psi}_\mathrm{m};\mathbf{x}_\mathrm{r})}{\partial\mathbf{x}_\mathrm{r}}\right)\right\}, \tag{7}$$

where $\mathrm{E}\{\cdot\}$ denotes the expectation operation and

$$\mathcal{L}(\boldsymbol{\psi}_\mathrm{m};\mathbf{x}_\mathrm{r}) = -\frac{1}{2}\ln\left(\det(2\pi\mathbf{W}_\psi)\right) - \frac{1}{2}(\boldsymbol{\psi}_\mathrm{m} - \boldsymbol{\psi}(\mathbf{x}_\mathrm{r}))^T\,\mathbf{W}_\psi^{-1}(\boldsymbol{\psi}_\mathrm{m} - \boldsymbol{\psi}(\mathbf{x}_\mathrm{r})) \tag{8}$$

is the log-likelihood function. Inserting (8) into (7), performing the expectation operation, and using the noise covariances in Section 2.2, we obtain the FIMs

$$\begin{aligned}\mathbf{J}_\alpha(\mathbf{x}_\mathrm{r}) &= \frac{1}{\sigma_\alpha^2}\sum_{i=1}^{N}\left(\frac{\partial\alpha(t_i)}{\partial\mathbf{x}_\mathrm{r}}\right)^T\frac{\partial\alpha(t_i)}{\partial\mathbf{x}_\mathrm{r}},\\ \mathbf{J}_{\dot\alpha}(\mathbf{x}_\mathrm{r}) &= \frac{1}{\sigma_{\dot\alpha}^2}\sum_{i=1}^{N}\left(\frac{\partial\dot\alpha(t_i)}{\partial\mathbf{x}_\mathrm{r}}\right)^T\frac{\partial\dot\alpha(t_i)}{\partial\mathbf{x}_\mathrm{r}}\end{aligned} \tag{9}$$

for the measurements of the azimuth ($\boldsymbol{\psi}_\mathrm{m} = \boldsymbol{\alpha}_\mathrm{m}$) and the azimuth rate ($\boldsymbol{\psi}_\mathrm{m} = \dot{\boldsymbol{\alpha}}_\mathrm{m}$). It is important to emphasize that the above given FIMs denote the maximum achievable information at an arbitrary reference time t_r based on N measurements. Finally, the CRBs read $\mathbf{J}_\alpha^{-1}(\mathbf{x}_\mathrm{r})$ and $(\mathbf{J}_\alpha(\mathbf{x}_\mathrm{r}) + \mathbf{J}_{\dot\alpha}(\mathbf{x}_\mathrm{r}))^{-1}$ for the azimuth-only case and the case using both azimuth and azimuth rate.

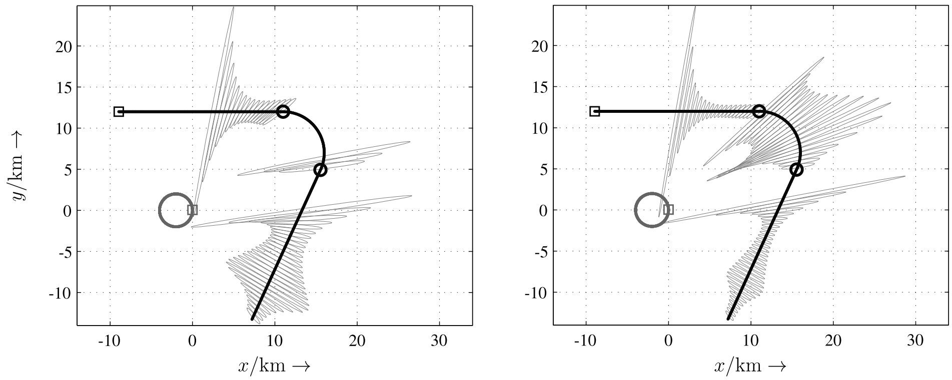

Figure 2: Observer path (green) with starting point (green square); target trajectory (blue) with target starting point (blue square) and target maneuver change-over points (blue circles). *Left*: CRB for the azimuth-only case (red ellipses). *Right*: CRB for combined azimuth and azimuth rate measurements (red ellipses).

4 Simulation results

We consider the 2D scenario in Fig. 2. The target starts with the initial state $(-9\,\mathrm{km}, 12\,\mathrm{km}, 50\,\mathrm{m/s}, 90°)^T$ and performs the following maneuvers:

$$\begin{aligned}(t_0, a_{\mathrm{t},0}, a_{\mathrm{n},0}) &= (0\,\mathrm{s}, 0\,\mathrm{m/s^2}, 0\,\mathrm{m/s^2})\,,\\ (\tilde{t}_1, a_{\mathrm{t},1}, a_{\mathrm{n},1}) &= (400\,\mathrm{s}, 0\,\mathrm{m/s^2}, 0.5\,\mathrm{m/s^2})\,,\\ (\tilde{t}_2, a_{\mathrm{t},2}, a_{\mathrm{n},2}) &= (600\,\mathrm{s}, 0\,\mathrm{m/s^2}, 0\,\mathrm{m/s^2})\,.\end{aligned}$$

The observer moves counterclockwise along a circular path with constant velocity. This is parameterized by $\mathbf{r}_\mathrm{O}(t_0) = (0\,\mathrm{km}, 0\,\mathrm{km})^T$, $|\dot{\mathbf{r}}_\mathrm{O}(t_0)| = 50\,\mathrm{m/s}$, $\varphi_\mathrm{O}(t_0) = 0°$, and $a_{\mathrm{O,n}} = -1.25\,\mathrm{m/s^2}$. The sensor collects one measurement per second, where the measurement noise is zero-mean Gaussian distributed with covariances given in Section 2.2. The corresponding standard deviations are $\sigma_\alpha = 2°$ and $\sigma_{\dot\alpha} = 1\,\mathrm{mrad/s}$ which are similar to the assumptions in [W$^+$08].

In Fig. 2, the results of the Cramér-Rao analysis are given. The bounds are illustrated by means of $90\,\%$ confidence ellipses. In the left part of the figure the CRB for the azimuth-only case are depicted, whereas in the right part of the figure the CRB for the combination of azimuth and azimuth rate measurements are shown. Note that for visualization purposes, ellipses have been drawn every $10\,\mathrm{s}$ and ellipses with an extent of over $30\,\mathrm{km}$ have been omitted.

It can be recognized that for all three legs of the target motion the estimation accuracy for the combined azimuth and azimuth rate case (right) is higher and converges faster than for azimuth-only measurements (left). Especially for the turn motion in the middle leg, reasonable estimation accuracies can be given for the combined azimuth/azimuth rate case, whereas azimuth-only measurements provide only inferior accuracies. Additionally, in Fig. 2, a decreasing estimation accuracy can be seen after a maneuver has taken place which is due to the dimension change of the target state at this time.

5 Conclusions

The considered target motion model subsumes the models described in the literature. We have presented an exact solution of the corresponding motion equation and have derived the CRB for the case that the maneuver accelerations and change-over times are unknown. In a Cramér-Rao analysis, we have found that the extension of the target state by acceleration components and change-over times leads to a declined estimation accuracy. Nevertheless, the achievable estimation accuracy can be significantly improved by using additional azimuth rate measurements.

References

[Bec96] K. Becker. A General Approach to TMA Observability from Angle and Frequency Measurements. *IEEE Trans. Aerosp. Electron. Syst.*, 32:487–494, January 1996.

[Bec01] K. Becker. Target Motion Analysis (TMA). In S. Stergioulos, editor, *Advanced Signal Processing Handbook*, chapter 9, pages 284–301. CRC Press, New York, NY, 2001.

[Bec05] K. Becker. Passive Aufklärung manövrierender Ziele aus Winkel- und Frequenzmessungen. FKIE Report 95, Research Establishment of Applied Science (FGAN), Wachtberg, April 2005. In German language.

[BN97] R. A. Best and J. P. Norton. A New Model and Efficient Tracker for a Target with Curvilinear Motion. *IEEE Trans. Aerosp. Electron. Syst.*, 33:1030–1037, July 1997.

[MBS05] W. Montlouis, O. Bayat, and B. Shafai. DOA and Angular velocity estimation using planar array with subspace based initialization. In *Proc. IEEE Military Communications Conference (MILCOM)*, pages 2797 – 2801, Atlantic City, NJ, October 2005.

[OH10] M. Oispuu and J. Hörst. Azimuth-only Localization and Accuracy Study for Piecewise Curvilinearly Moving Targets. In *Proc. ISIF 13th International Conference on Information Fusion*, Edinburgh, UK, July 2010. To be published.

[RA03] B. Ristic and M. S. Arulampalam. Tracking a manoeuvring target using angle-only measurements: algortihms and performance. *IEEE Trans. Signal Processing*, 83:1223–1238, 2003.

[RAG04] B. Ristic, M. S. Arulampalam, and N. Gordon. *Beyond the Kalman Filter: Particle Filters for Tracking Applications*. Artech House, Boston, MA, 2004.

[W$^+$08] J. Wang et al. Passive Location to Moving Emitter Using DOA and Its Rate of Change. *Congress on Image and Signal Processing 2008 (CISP'08)*, 4, 2008.

[WE95] T. Wigren and A. Eriksson. Accuracy Aspects of DOA and Angular Velocity Estimation in Sensor Array Processing. *IEEE Signal Processing Lett.*, 2:60–62, April 1995.